Supplemental Information

eMethods

Questionnaires

Difficulties in Emotion Regulation – Impulse Control Subscale (DERS-Impulse Control; (Gratz and Roemer, 2004): The DERS is a 36-item self-report measure used to assess manifestations of emotion dysregulation across six domains. The Impulse Control Subscale is particularly pertinent to the current investigation by tapping into executive inhibition when distressed. The Impulse Control Subscale consists of 6 items on a 5-point Likert scale (e.g., "When I am upset, I become out of control"), ranging from 1 (Almost never) to 5 (Almost always). The DERS and its subscales have strong internal consistency and construct validity within both clinical and nonclinical samples (Gratz and Roemer, 2004).

Posttraumatic Stress Disorder Checklist for DSM-IV – Civilian Version (PCL-C; (Blanchard et al., 1996)): The PCL-C is a 17-item, self-report measure assessing severity of PTSD symptoms across the 4 symptom clusters: Intrusion (items 1 through 5), Avoidance (items 6 through 7), Negative Alterations in Mood and Cognition (items 8 through 12), and Hyperarousal (items 13 through 17). Participants indicate how much they have been bothered by the particular symptom over the past month on a 5-point Likert Scale from 1 (Not at all) to 5 (Extremely). Item 16 assessing symptoms of hypervigilance or "being watchful or on guard" was used to index hypervigilance. In the present study, internal consistency was high for the total questionnaire ($\alpha = .95$), as well as the individual Hyperarousal cluster ($\alpha = .84$), in accordance with past work

demonstrating strong psychometric properties of the PCL-C in both clinical and non-clinical populations (Wilkins *et al.*, 2011).

Beck Anxiety Inventory (BAI; (Beck et al., 1988a)): The BAI is a 21-item self-report measure of general physical/somatic and cognitive symptoms of anxiety. Responses are made to the extent each symptom has bothered the respondent in the past week on a scale from 0 (Not at all) to 3 (Severely). The BAI is highly reliable in both clinical ($\alpha = .92$) and nonclinical ($\alpha = .91$) samples (Beck *et al.*, 1988a; Borden *et al.*, 1991).

State and Trait Anxiety Inventory – Trait (STAI-T; (Spielberger, 1983)): The STAI-T is a 20-item self-report measure of a general propensity to be anxious. It has been demonstrated to be sensitive to negative affect not specific to anxiety (Bieling *et al.*, 1998). Responses are indicative of the frequency the respondent generally experiences these symptoms across no specified timeframe, ranging from 1 (Almost never) to 4 (Almost always). The STAI demonstrates high test-retest reliability (0.73-0.86) and concurrent validity with other anxiety questionnaires (0.73-0.85; (Spielberger, 1983)).

Beck Depression Inventory– 2nd Edition (BDI-II; (Beck et al., 1988b)): The BDI-II is a 21-item self-report measure assessing the severity of depressive symptoms. Responses are made to the extent the respondent has experienced and been bothered by the symptoms in the past two weeks, ranging from 0 (e.g. “I do not feel sad”) to 3 (e.g. “I am so sad or unhappy that I can’t stand it”). The BDI-II demonstrates high internal consistency in outpatient populations ($\alpha = .92$; (Beck *et al.*, 1996)) and discriminative validity with the BAI (Creamer *et al.*, 1995).

A main effect of group emerged for all the questionnaires (F's > 4.5, *p*'s <.05). PTSD and GAD groups showed higher scores compared to the HC group (*p*'s < .05) in all questionnaires, except for DERS-Impulse Control, which was specifically elevated in PTSD (GAD vs. HC, *p* = .06). The PTSD group showed further elevations on the BAI, PCL total, PCL-Hyperarousal cluster, and PCL-Hypervigilance symptom, compared to the GAD group (*p*'s < .005).

Images

In the modified resting state (M-RS), a succession of 921 pictures were continuously presented at the center of the monitor (subtending a visual area of 7.8° X 5.8°), each for 333 ms, using E-Prime (Psychology Software Tools, 2012). Images were chosen from the International Affective Picture System (Lang *et al.*, 2008), consisting of 322 neutral (e.g. buildings, daily objects), 253 positive (e.g. erotic), and 346 negative (e.g. mutilation), randomly intermixed.

FASTER Algorithm

The *Fully Automated Statistical Thresholding for EEG artifact Rejection* (FASTER) algorithm (Nolan *et al.*, 2010) was used for the detection and removal of artifacts within the data. Using a z-score threshold of ± 3, the FASTER algorithm detects and corrects for artifacts within single channels, individual epochs, independent components, and within-epoch channels. FASTER first interpolates deviant channels from the continuous data using the EEGLAB spherical spline interpolation function. Data were then segmented into non-overlapping, 1-second long, mean-centered epochs. Epochs were then rejected based on Z-scores of ± 3 within parameters of amplitude range, variance, and deviation. Epoched data were then re-referenced to

averaged mastoids and submitted to independent component analysis (ICA) decomposition using the Infomax algorithm (Bell and Sejnowski, 1995). Artefactual components (i.e. muscular artifacts, eye blinks and saccades, electrode "pop-offs", etc.) were automatically detected and removed from the data. Lastly, deviant channels within individual, cleaned epochs were interpolated again using the EEGLAB spherical spline interpolation function.

Exact low resolution brain electromagnetic tomography (eLORETA)

To ascertain cortical sources of alpha and gamma oscillations, we conducted intracranial source analysis based on scalp power values using eLORETA (Pascual-Marqui *et al.*, 2011). The eLORETA has been cross-validated with functional magnetic resonance imaging (fMRI) data (Pascual-Marqui *et al.*, 2011; Neuner *et al.*, 2014; Aoki *et al.*, 2015). The eLORETA applies a weighted minimum norm inverse solution, where the weights are unique and thus allow for exact localization for any point source in the brain, even in the presence of structured noise. In this sense, eLORETA is an improvement over earlier versions of LORETA (which has been cross-validated with functional magnetic resonance imaging (fMRI) data; (Pascual-Marqui *et al.*, 1994) and sLORETA (Pascual-Marqui *et al.*, 2002). The eLORETA solution space is based on a three-shell spherical head model (Fuchs *et al.*, 2002) registered to standardized space from a digitized MRI at the Montreal Neurological Institute (MNI), restricted to cortical gray matter, spanning 6239 voxels with a spatial resolution of 5x5x5 mm^3.

Granger Causality

To mitigate adverse effects of volume conduction and shared electrical source on connectivity analyses (Srinivasan *et al.*, 2007), we first transformed scalp data into reference-

free, current source density (CSD) data using the surface Laplacian algorithm (Perrin *et al.*, 1989). Granger causality (GC) analysis (Geweke, 1982; Ding *et al.*, 2000) was performed on the AR modeled CSD data.

GC is a measure of causal connectivity based on time-series prediction (Geweke, 1982; Ding *et al.*, 2000), or the extent to which one signal, *Y,* is influenced by past values of a different signal, *X*. GC is quantified by how much better one signal predicts the values of a different signal than previous values of that same signal. Given two, bivariate autoregressive processes, characterized as,

$$X_t = \sum_{n=1}^{k} a_n X_{t-n} + b_n Y_{t-n} + e_{xyt}$$

$$Y_t = \sum_{n=1}^{k} c_n Y_{t-n} + d_n X_{t-n} + e_{yxt}$$

GC from signal X to Y can be quantified as,

$$GC_{X \rightarrow Y} = \ln\left(\frac{var(e_y)}{var(e_{xy})}\right)$$

where var(e_{xy}) is the error variance of the bivariate autoregressive model between signals X and Y, and var(e_y) is the error variance of the univariate autoregressive process within signal Y alone. Thus, the better signal X predicts signal Y, the smaller the bivariate error term variance, and thus the greater GC.

Supplemental Analyses

Comparisons between PTSD and traumatized non-PTSD groups

To rule out potential trauma-related confounds in our findings, we further compared the PTSD group with a control group of traumatized non-PTSD subjects (n = 20). This control group consisted of 7 subjects from both of the GAD and HC groups and 6 additional subjects. All these

patients had prior trauma exposure (meeting the PTSD diagnosis Criterion A) but did not meet criteria for a diagnosis of PTSD based on the SCID. These additional 6 subjects (mean age: 42.1 years; range: 26-52 years; all male) had no history of severe neurological disorders or traumatic brain injury, no current or past psychotic-spectrum or bipolar disorders, and no current substance dependence or abuse of opioids, stimulants, or cocaine. Three of the six subjects did not have a current diagnosis, one had a diagnosis of persistent depression disorder, and two had a diagnosis of mild alcohol use disorder. Respective repeated-measures ANOVAs were conducted on posterior alpha power, frontal gamma power, and alpha GC during the standard resting state (a passive picture viewing condition was not administered in the six new subjects), with substance use as a covariate.

Posterior alpha power: An ANOVA (Group X Site) revealed a main effect of group ($F_{1, 41} = 11.22$, $p = .002$, $\eta_p^2 = .22$). The PTSD group demonstrated significantly reduced posterior alpha power compared to the traumatized control group [mean (SD): PTSD = 2.26 (0.91); traumatized non-PTSD = 3.45 (1.35)]. There was a significant site-by-group interaction ($F_{1.75, 71.62} = 3.47$, $p = .042$, $\eta_p^2 = .08$), substantiated by a main effect of site in the traumatized control group ($F_{1.69, 30.44} = 4.26$, $p = .028$, $\eta_p^2 = .11$). No such effect of site was seen in the PTSD group ($F_{1.84, 40.42} = .19$, $p = .813$).

Frontal gamma power: An ANOVA (Group X Site) revealed a main effect of group ($F_{1, 41} = 5.21$, $p = .028$, $\eta_p^2 = .11$), characterized by heightened frontal gamma activity in the PTSD group [0.49 (.25)] compared to the traumatized non-PTSD group [0.33 (0.16)]. There were no other significant effects (p's > .1).

Alpha-GC: An ANOVA (Group X Hemisphere X Direction) revealed a main effect of group ($F_{1, 41}$ = 8.34, p = .006, η_p^2 = .17), characterized by reduced GC in the PTSD group [0.02 (0.01)] relative to the traumatized non-PTSD group [0.03 (0.02)]. A three-way interaction of direction-by-hemisphere-by-group was also revealed ($F_{1, 41}$ = 6.37, p = .016, η_p^2 = .13). A follow-up ANOVA (Group X Direction) in the left hemisphere showed no significant effects (p's > .114). A similar ANOVA in the right hemisphere demonstrated a main effect of group [$F_{1, 41}$ = 9.00, p = .005, η_p^2 = .18; PTSD = 0.02 (0.01); traumatized non-PTSD = 0.03 (0.03)]. There was also a direction-by-group interaction ($F_{1, 41}$ = 5.86, p = .020, η_p^2 = .13), such that the PTSD group (vs. traumatized non-PTSD group) demonstrated deficient bottom-up GC [$F_{1, 41}$ = 7.94, p = .007, η_p^2 = .16; PTSD = 0.02 (0.01); traumatized non-PTSD = 0.05 (0.05)], but only a non-significant trend in top-down GC [$F_{1, 41}$ = 1.78, p = .189; PTSD = 0.01 (0.01); traumatized non-PTSD = 0.02 (0.01)].

In conclusion, ANOVAs on all three key measures demonstrated significant group effects, which closely conformed to the main analyses reported in the main text and thus ruled out the trauma-related confound.

Mu effects

Although the posterior alpha oscillations are by far the strongest across the entire scalp, mu oscillations (a somatosensory analogue of the visual alpha activity) could also be accessed via scalp EEG recordings and so were considered to reflect somatosensory anomalies in PTSD. We extracted mu oscillations (8-12 Hz) from bilateral central sites (Supplemental Figure 1; Yin *et al.*, 2016) and submitted the values to an ANOVA (Group X State X Site). Similar to the

posterior alpha effects, we observed a main effect of group ($F_{2, 60} = 4.18$, $p = .020$, $\eta_p^2 = .12$), characterized by suppressed mu power in the PTSD group [1.86 (0.50)], relative to the GAD [2.52 (0.86); $t_{42} = -2.62$, $p = .011$, $d = 0.81$] and the HC groups [2.49 (0.96); $t_{38} = -2.49$, $p = .016$, $d = 0.81$]. These follow-up contrasts survived the corrected $p < .05$ FDR. No other effects were significant (p's > .1).

Supplemental References

Aoki Y, Ishii R, Pascual-Marqui RD, Canuet L, Ikeda S, Hata M, *et al.* Detection of EEG-resting state independent networks by eLORETA-ICA method. Front Hum Neurosci 2015; 9: 31.

Beck AT, Epstein N, Brown G, Steer RA. An inventory for measuring clinical anxiety: psychometric properties. J Consult Clin Psychol 1988a; 56(6): 893-7.

Beck AT, Steer RA, Ball R, Ranieri W. Comparison of Beck Depression Inventories -IA and -II in psychiatric outpatients. J Pers Assess 1996; 67(3): 588-97.

Beck AT, Steer RA, Carbin MG. Psychometric properties of the Beck Depression Inventory: Twenty-five years of evaluation. Clinical Psychology Review 1988b; 8(1): 77-100.

Bell AJ, Sejnowski TJ. An information-maximization approach to blind separation and blind deconvolution. Neural computation 1995; 7(6): 1129-59.

Bieling PJ, Antony MM, Swinson RP. The State-Trait Anxiety Inventory, Trait version: structure and content re-examined. Behav Res Ther 1998; 36(7-8): 777-88.

Blanchard EB, Jones-Alexander J, Buckley TC, Forneris CA. Psychometric properties of the PTSD Checklist (PCL). Behav Res Ther 1996; 34(8): 669-73.

Borden KL, Beckmann P, Lane AN. Determination of the orientations of tryptophan analogues bound to the trp repressor and the relationship to activation. Eur J Biochem 1991; 202(2): 459-70.

Creamer M, Foran J, Bell R. The Beck Anxiety Inventory in a non-clinical sample. Behav Res Ther 1995; 33(4): 477-85.

Ding M, Bressler SL, Yang W, Liang H. Short-window spectral analysis of cortical event-related potentials by adaptive multivariate autoregressive modeling: data preprocessing, model validation, and variability assessment. Biol Cybern 2000; 83(1): 35-45.

Fuchs M, Kastner J, Wagner M, Hawes S, Ebersole JS. A standardized boundary element method volume conductor model. Clin Neurophysiol 2002; 113(5): 702-12.

Geweke J. Measurement of linear dependence and feedback between multiple time series. Journal of the American statistical association 1982; 77(378): 304-13.

Gratz KL, Roemer L. Multidimensional assessment of emotion regulation and dysregulation: Development, factor structure, and initial validation of the difficulties in emotion regulation scale. J Psychopathol Behav 2004; 26(1): 41-54.

Lang P, Bradley M, Cuthbert BN. International affective picture system (IAPS): Affective ratings of pictures and instruction manual; 2008.

Neuner I, Arrubla J, Werner CJ, Hitz K, Boers F, Kawohl W, *et al.* The default mode network and EEG regional spectral power: a simultaneous fMRI-EEG study. PLoS One 2014; 9(2): e88214.

Nolan H, Whelan R, Reilly RB. FASTER: Fully Automated Statistical Thresholding for EEG artifact Rejection. J Neurosci Methods 2010; 192(1): 152-62.

Pascual-Marqui RD, Esslen M, Kochi K, Lehmann D. Functional imaging with low-resolution brain electromagnetic tomography (LORETA): a review. Methods Find Exp Clin Pharmacol 2002; 24 Suppl C: 91-5.

Pascual-Marqui RD, Lehmann D, Koukkou M, Kochi K, Anderer P, Saletu B, *et al.* Assessing interactions in the brain with exact low-resolution electromagnetic tomography. Philos Trans A Math Phys Eng Sci 2011; 369(1952): 3768-84.

Pascual-Marqui RD, Michel CM, Lehmann D. Low resolution electromagnetic tomography: a new method for localizing electrical activity in the brain. Int J Psychophysiol 1994; 18(1): 49-65.

Perrin F, Pernier J, Bertrand O, Echallier JF. Spherical splines for scalp potential and current density mapping. Electroencephalogr Clin Neurophysiol 1989; 72(2): 184-7.

Psychology Software Tools I. E-Prime 2.0. Pittsburgh: Psychology Software Tools, Inc.; 2012.

Spielberger CDG, R.L.; Lushene, R;, Vagg, P.R.; & Jacobs, G.A. Manual for the State-Trait Anxiety Inventory. Palo Alto, CA: Consulting Psychologists Press; 1983.

Srinivasan R, Winter WR, Ding J, Nunez PL. EEG and MEG coherence: measures of functional connectivity at distinct spatial scales of neocortical dynamics. J Neurosci Methods 2007; 166(1): 41-52.

Wilkins KC, Lang AJ, Norman SB. Synthesis of the Psychometric Properties of the Ptsd Checklist (Pcl) Military, Civilian, and Specific Versions. Depression and Anxiety 2011; 28(7): 596-606.

Yin S, Liu Y, Ding M. Amplitude of Sensorimotor Mu Rhythm Is Correlated with BOLD from Multiple Brain Regions: A Simultaneous EEG-fMRI Study. Front Hum Neurosci 2016; 10: 364.

Table S1 Summary of results pertinent to hypothesis testing

	Alpha Power	**Gamma Power**	**Alpha GC**
Hypotheses	PTSD < GAD/HD	PTSD > GAD/HD	PTSD < GAD/HD
ANOVA group effects	$F = 3.96$, $p = .024$	$F = 2.48$, $p = .093$	$F = 5.21$, $p = .008$
	Effect size: $\eta_p^2 = .12$	Effect size: $\eta_p^2 = .08$	Effect size: $\eta_p^2 = .15$
Contrast—PTSD vs. GAD	$t = -2.37$, $p = .021$ uncor. $p < .05$ FDR	$t = 2.16$, $p = .037$ uncor. $p < .05$ FDR*	$t = -2.89$, $p = .006$ uncor. $p < .05$ FDR
	Effect size: $d = .75$	Effect size: $d = .67$	Effect size: $d = .85$
Contrast—PTSD vs. HC	$t = -2.58$, $p = .012$ uncor. $p < .05$ FDR	$t = 1.98$, $p = .055$ uncor. $p < .05$ FDR*	$t = -2.95$, $p = .006$ uncor. $p < .05$ FDR
	Effect size: $d = .82$	Effect size: $d = .64$	Effect size: $d = .90$
Conclusion	✓	✓	✓

Note: Interaction effects across group, state, site and direction are detailed in the text. *= one-tailed test.

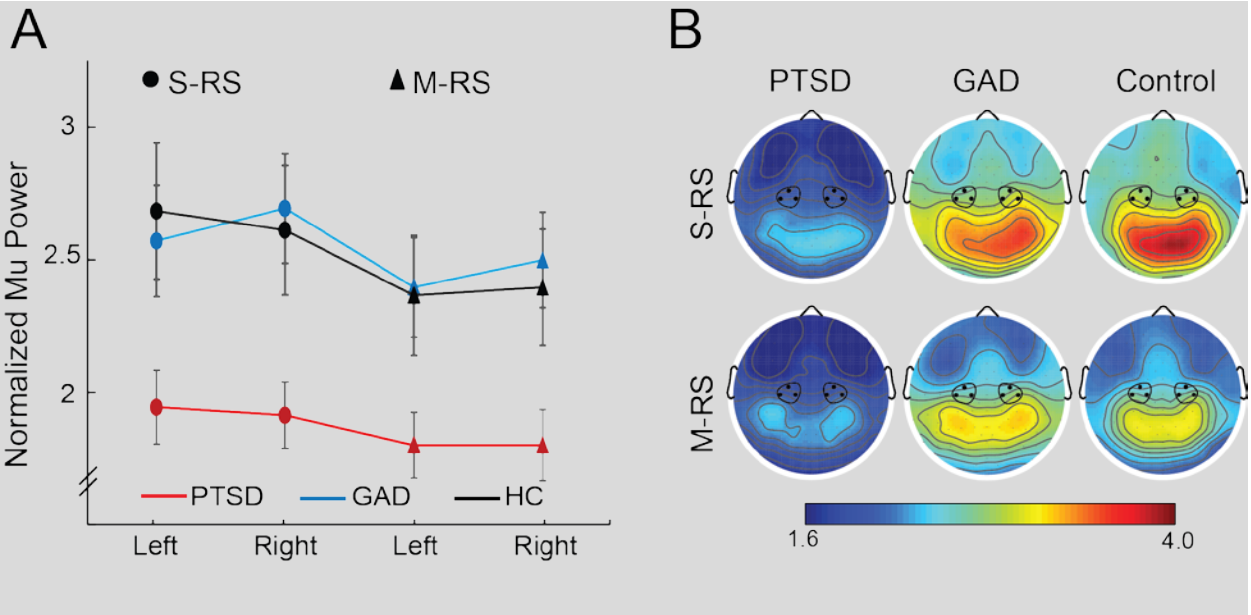

Supplemental Figure 1. Central mu power. **(A)** Mu power magnitudes at left and right central sites. Error bars = S.E.M. **(B)** Scalp topographical maps of 8-12 Hz power, with electrodes included in central (sensory-motor) sites bolded and circled.